R. & M. No. 3544

MINISTRY OF TECHNOLOGY

AERONAUTICAL RESEARCH COUNCIL
REPORTS AND MEMORANDA

# The Stability of Rotor Blade Flapping Motion at High Tip Speed Ratios

By O. J. LOWIS



LONDON: HER MAJESTY'S STATIONERY OFFICE
1968

PRICE 12*s*. 6*d*. NET

# The Stability of Rotor Blade Flapping Motion at High Tip Speed Ratios

By O. J. Lowis

*Reports and Memoranda No.* 3544*
*January*, 1963

*Summary.*

In this Report a method of obtaining the transient solution of the helicopter rotor blade flapping motion is developed and the effective damping of the motion determined for tip speed ratios up to unity and above.

When reverse flow over the retreating blade is ignored, it is found that the motion becomes unstable in the region of tip speed ratios of $\sqrt{2}$ for values of inertia number up to 2. However when the equation of motion is modified to take into account the reverse flow over the retreating blade, the flapping motion becomes unstable at tip speed ratios between 2·2 and 2·8.

Use is made of a digital computer in performing the numerical processes necessary to the method, which could be applied to solving other linear differential equations with periodic coefficients.

CONTENTS



*Replaces A.R.C. 23 371.

## 1. *Introduction.*

Previous papers by Horvay[1], Shutler and Jones[2], and Horvay and Yuan[3], have dealt with the problem of the transient flapping motion of a helicopter rotor blade in forward flight. These papers consider the problem for relatively low tip speed ratios $\mu$ from 0 to 0·6 and show, in general, that as $\mu$ increases regions of destabilization (i.e. regions where the flapping motion is less stable than that in hovering conditions) develop. In these regions of destabilization the frequency of oscillation is either $\frac{1}{2}$ or 1 depending on the physical and aerodynamic properties of the blade, and over the range of $\mu$ considered, the flapping motion therein becomes less stable as the tip speed ratio increases.

Now future developments in helicopter engineering may involve flight where the tip speed ratios are much larger than those encountered at present, and under these circumstances it is necessary to examine the nature of the rotor blade flapping motion for values of $\mu$ up to unity and higher.

The methods used in the papers referred to above, however, are not applicable to solving the problem for high tip speed ratios because the equation of motion considered therein does not take into account the reverse flow over the retreating blade, the effect of which increases with increasing $\mu$. Moreover the methods of Horvay[1], and Shutler and Jones[2], derive solutions by ignoring high powers of $\mu$ and therefore cannot be used when considering values of unity and higher.

The purpose of this report, therefore, is to present a method of solution which will extend the results of these previous papers into higher regions of tip speed ratio and to show whether or not the decrease in stability continues as $\mu$ increases. This method which is described fully in a thesis by Lowis[4] is similar in approach to that of Horvay and Yuan[3], but the use of a digital computer enables a more detailed treatment to be undertaken.

For the problem of solving the blade flapping equation when reverse flow is not taken into account, it may be argued that if the steady state solution is assumed to be of the form

$$\beta = a_0 + \sum_{r=1}^{\infty} a_r \cos r\omega t + b_r \sin r\omega t,$$

the coefficient $a_1$ is found to be given by the equation

$$(1-\tfrac{1}{2}\mu^2)a_1 \doteq -(\tfrac{2}{3}\mu b_2+\tfrac{1}{2}\mu^2 a_3)+\mu\delta,$$

where $\delta$ is a function of flight conditions, suggesting that resonance occurs when $\mu = \sqrt{2}$, and indicating in turn that this is a value of tip speed ratio giving instability.

However the equation for $a_1$ is effectively obtained by expanding in powers of $\mu$ and retaining a finite number of terms. This in itself implies that an approximation is being made and that a further investigation is required to confirm that instability occurs when $\mu = \sqrt{2}$. Moreover $a_1$ is the coefficient of the first harmonic ($\cos \omega t$) term in the series for $\beta$ and as such the instability would be expected to occur in the region of destabilization where the frequency is 1. For low tip speed ratios this region is relatively small, and previous investigations for low $\mu$ would appear to indicate that the region of destabilization with frequency $\frac{1}{2}$ is the least stable. Therefore before the significance of this instability can be fully realised it is necessary to see how these regions develop as $\mu$ increases.

The first part of this Report, therefore, deals with the problem of solving the blade flapping equation when reverse flow is ignored. While this may be somewhat unrealistic at high tip speed ratios, in so far as it no longer represents the time blade motion, it serves to illustrate the basic method adopted herein, and also answers the questions as to how the regions of destabilization develop as $\mu$ increases past 0·6, and whether or not instability of the system represented by this equation does eventually occur.

In the second part of the Report, Section 6 *et seq.*, this method is then applied to the equation of motion which is derived when reverse flow is taken into account.

It will be shown in general, that the initial increase in area of regions of destabilization as $\mu$ increases, already demonstrated in previous papers, continues. When reverse flow effects are ignored the motion of the blade becomes unstable at $\mu = \sqrt{2}$. When allowance is made for reverse flow, however, the onset of instability is delayed until higher values of $\mu$ are reached.

## 2. *The Equation of Flapping Motion.*

For simplicity it is assumed that the blade is untwisted, of constant chord and does not bend or twist. The flapping hinge is assumed to be on the axis of rotation and perpendicular to the spanwise axis of the blade, i.e., $\delta_3 = 0$. At this stage we assume that there is no region of reverse flow over the retreating blade.

By considering the moments about the flapping hinge of all forces acting on a helicopter rotor blade, the equation of flapping motion is found to be[1]

$$\frac{d^2\beta}{dt^2} + 2C(t)\frac{d\beta}{dt}+P^2(t)\beta = E(\omega t) \qquad (1)$$

where

$$2C(t) = n\omega\left[1+\frac{4}{3}\mu\sin\omega t\right]$$

$$P^2(t) = \omega^2\left[1+\frac{4n\mu}{3}\cos\omega t+n\mu^2\sin 2\omega t\right]$$

and $E(\omega t)$ is an aerodynamic forcing function independent of $\beta$. The transient motion is given by the solution to the equation

$$\frac{d^2\beta}{dt^2}+2C(t)\frac{d\beta}{dt}+P^2(t)\beta = 0 \qquad (2)$$

and it is this solution which concerns us initially in this Report.

## 3. *Preliminary Theorems.*

In this Section we state without proof and discuss briefly two results, and prove one further result, all of which are used later in Section 5.

### 3.1. *Floquet's Theorem*

Any linear differential equation of the second order, having periodic coefficients of period $2\pi$ and which are functions of time $t$, has a transient solution[5] of the form

$$\alpha_1 \exp[\gamma_1 t].P_1(t) + \alpha_2 \exp[\gamma_2 t].P_2(t) \tag{3}$$

where $\gamma_1$, $\gamma_2$ are constants (not necessarily real) and $P_1(t)$, $P_2(t)$ are periodic functions of time of period $2\pi$. $\alpha_1$, $\alpha_2$ are arbitrary constants depending on the initial conditions.

We note that as $P_1(t)$ and $P_2(t)$ are periodic functions, the stability of the motion depends on the real part of $\gamma_1$ and $\gamma_2$. The main objective therefore is to evaluate the real part of $\gamma_1$ or $\gamma_2$, the one having the most positive value being the critical one.

### 3.2. *Instability Regions and Characteristic Curves.*

A discussion[5] of an equation of Hill's type

i.e.,
$$\ddot{x} + [a - 2qF(\omega t)]x = 0 \tag{4}$$

where $F(\omega t)$ is periodic shows that the $a$, $q$ plane is divided into regions where the solutions are stable or unstable, these regions being separated by what are called characteristic curves. Horvay[1] reduces the rotor blade flapping equation to this form and the results show that the $\mu$, $n$ plane (equivalent to the $a$, $q$ plane) is divided into similar regions where the solution is stable or unstable. As equation (4) is a linear differential equation of the second order with periodic coefficients, it has a solution of the form (3) and it is shown that each term of the expression represents a damped (positively or negatively) periodic function with constant frequency for a given instability region. In particular for the type of equation given by (4) it is shown that

$$\gamma_1 = -\gamma_2. \tag{5}$$

### 3.3. *Solution using Matrix Equations.*

We now show that if $[y]$ and $[x]$ are column vectors with $n$ elements and $[M]$ is an $n \times n$ square matrix and if both

$$[y] = [M][x]$$

and

$$[y] = [\Lambda I][x]$$

where $[I]$ is the unit matrix, then $\Lambda$ is given by the latent roots of $[M]$.

*Proof*

Clearly
$$[M][x] = [\Lambda I][x]$$
i.e.,
$$[M - \Lambda I][x] = 0. \tag{6}$$

The condition that the $n$ equations written in matrix form by equation (6) are consistent is that,

$$|M - \Lambda I| = 0.$$

Thus $\Lambda$ is given by the latent roots of $[M]$.

4. *Method of Solution.*

We now proceed to describe a method of solving equation (2).

4.1. *Reduction of Flapping Equation to Hill Equation.*

Equation (2) can be written

$$\frac{d^2\beta}{d\psi^2}+n\left(1+\frac{4}{3}\mu\sin\psi\right)\frac{d\beta}{d\psi}+\left(1+\frac{4}{3}n\mu\cos\psi+n\mu^2\sin 2\psi\right)\beta = 0 \tag{7}$$

where $\psi = \omega t$ is the azimuth angle of the rotor blade. Writing

$$\beta = \exp\left[-\frac{n}{2}\psi+\frac{2}{3}n\mu\cos\psi\right].v(\psi) \tag{8}$$

equation (7) reduces to

$$v''+Q^2(\psi)v = 0 \tag{9}$$

where the dashes denote differentiation with respect to $\psi$ and

$$Q^2(\psi) = \left(1-\frac{n^2}{4}-\frac{2}{9}n^2\mu^2+\frac{2}{3}n\mu\cos\psi-\frac{2}{3}n^2\mu\sin\psi+n\mu^2\sin 2\psi+\frac{2}{9}n^2\mu^2\cos 2\psi\right). \tag{10}$$

This is an equation of the type (4) where $Q^2(\psi)$ is periodic with period $2\pi$, and so by Section 4 it has a solution of the form

$$v = \alpha_1\exp[\gamma\psi].P_1(\psi)+\alpha_2\exp[-\gamma\psi].P_2(\psi) \tag{11}$$

where $P_1(\psi)$ and $P_2(\psi)$ are periodic functions of period $2\pi$ and where $\alpha_1$ and $\alpha_2$ are arbitrary constants.

Thus from equations (8) and (11) the solution to equation (7) is given by

$$\beta = \alpha_1\exp\left[-\left(\frac{n}{2}-\gamma\right)\psi\right].P_1(\psi)\exp\left[\frac{2}{3}n\mu\cos\psi\right]+\alpha_2\exp\left[-\left(\frac{n}{2}+\gamma\right)\psi\right]. \\ \times P_2(\psi)\exp\left[\frac{2}{3}n\mu\cos\psi\right] \tag{12}$$

and if we write $\gamma = \lambda+i\nu$ it is seen that the motion is stable or unstable according to whether $\lambda$ is less than or greater than $n/2$. Our main objective therefore, is to evaluate $\gamma$ and hence $\lambda$ in the solution of equation (9).

4.2. *The Rectangular Ripple Principle.*

The method of solution of equation (9) to be adopted here is to split one revolution of $\psi$, i.e., $\psi = 0$ to $\psi = 2\pi$, into short intervals $\psi_s-\psi_{s-1}$, over which the variable coefficients $Q^2(\psi)$ may be considered constant.

Since the values of $v$ and $v'$ must be continuous throughout successive intervals, the final values $v$ and $v'$ at the end of one interval are the initial values of the variables for the next interval.

We therefore approximate the actual equation (9) by a set of equations whose coefficients $Q^2$ are fixed throughout each of the short intervals $\psi_s-\psi_{s-1}$. The value of $Q^2$ for each interval is obtained by substituting the mean value of $\psi$ for the interval in $Q^2(\psi)$.

Assuming $Q$ is constant therefore, equation (9) has a solution

$$v(\psi) = A\cos Q\psi + B\sin Q\psi \tag{13}$$

so that

$$v'(\psi) = -QA\sin Q\psi + QB\cos Q\psi \tag{14}$$

$A$ and $B$ being constants determined from initial conditions for each interval. Equations (13) and (14) can be expressed by the matrix equations

$$[V(\psi)] = [M(\psi)][C] \tag{15}$$

where

$$[V(\psi)] = \begin{bmatrix} v(\psi) \\ v'(\psi) \end{bmatrix}$$

$$[M(\psi)] = \begin{bmatrix} \cos Q\psi & \sin Q\psi \\ -Q\sin Q\psi & Q\cos Q\psi \end{bmatrix}$$

and

$$[C] = \begin{bmatrix} A \\ B \end{bmatrix}.$$

Now if we divide one revolution of $\psi$ into $r$ equal intervals, then each interval is of magnitude $(2\pi/r)$ and the mean value for the $s^{th}$ interval is $(2s-1)\pi/r$. $Q_s$, the value of $Q(\psi)$ for the $s^{th}$ interval, is found by writing $\psi = (2s-1)\pi/r$, in equation (10) and then the values of $v$ and $v'$ in that interval are given by

$$[V_s(\psi)] = [M_s(\psi)][C_s]. \tag{16}$$

In this equation $\psi$ takes values $0 < \psi < \dfrac{2\pi}{r}$.

Now the arbitrary constants in $[C_s]$ are determined by the initial conditions which are that

$$[V_s(0)] = \left[V_{s-1}\left(\frac{2\pi}{r}\right)\right] \tag{17}$$

which is the condition that $v$ and $v'$ are continuous.

Thus

$$[V_s(0)] = [M_s(0)][C_s]$$

or

$$[C_s] = [M_s(0)]^{-1}[V_s(0)]$$

i.e.

$$[C_s] = [M_s(0)]^{-1}\left[V_{s-1}\left(\frac{2\pi}{r}\right)\right]. \tag{18}$$

Now given the initial conditions for the first interval, i.e. $v(0) = v_1(0)$, $v'(0) = v_1'(0)$ or $[V(0)] = [V_1(0)]$ we have from (16)

$$[V_1(\psi)] = [M_1(\psi)][C_1]$$

where from (18)

$$[C_1] = [M_1(0)]^{-1}[V_1(0)]$$

so that

$$[V_1(\psi)] = [M_1(\psi)][M_1(0)]^{-1}[V_1(0)]. \tag{19}$$

By writing $\psi = \frac{2\pi}{r}$ in equation (19) and using equation (17) we obtain

$$[V_2(0)] = \left[M_1\left(\frac{2\pi}{r}\right)\right] \; [M_1(0)]^{-1}[V_1(0)], \tag{20}$$

which gives the initial conditions for the second interval. Repeating this process for the second interval gives

$$[V_2(\psi)] = [M_2(\psi)][M_2(0)]^{-1}\left[M_1\left(\frac{2\pi}{r}\right)\right] \; [M_1(0)]^{-1}[V_1(0)]. \tag{21}$$

From this we obtain $\left[V_2\left(\frac{2\pi}{r}\right)\right]$ and hence $[V_3(0)]$ and so by repeated application of the progress we obtain

$$[V(2\pi)] = \left[V_r\left(\frac{2\pi}{r}\right)\right] = \prod_{s=r}^{1}\left[M_s\left(\frac{2\pi}{r}\right)\right] \; [M_s(0)]^{-1}.[V_1(0)] \tag{22}$$

where the order of multiplication of matrices is such that the product starts with $s = r$ and ends with $s = 1$.

Now $$[M_s(0)] = \begin{bmatrix} 1 & 0 \\ 0 & Q_s \end{bmatrix}$$

so $$[M_s(0)]^{-1} = \begin{bmatrix} 1 & 0 \\ 0 & 1/Q_s \end{bmatrix}$$

Hence

$$[\mathscr{M}_s] = \begin{bmatrix} \cos\left(Q_s\frac{2\pi}{r}\right) & \frac{1}{Q_s}\sin\left(Q_s\frac{2\pi}{r}\right) \\ -Q_s\sin\left(Q_s\frac{2\pi}{r}\right) & \cos\left(Q_s\frac{2\pi}{r}\right) \end{bmatrix} \tag{23}$$

where $$[\mathscr{M}_s] = \left[M_s\left(\frac{2\pi}{r}\right)\right] \; [M_s(0)]^{-1}.$$

Thus $$[V(2\pi)] = \prod_{s=r}^{1}[\mathscr{M}_s].[V(0)]. \tag{24}$$

But $$|\mathscr{M}_s| = 1 \text{ and hence we note that } \left|\prod_{s=r}^{1}[\mathscr{M}_s]\right| = 1. \tag{25}$$

We see therefore, that $v(2\pi)$ and $v'(2\pi)$ can be calculated in terms of $v(0)$ and $v'(0)$ by process of evaluating a series of matrix products involving all the $Q_s$'s. The $Q_s$'s are calculated and matrices formed and multiplied using a digital computer. (If $Q^2$ is negative in any interval then the trigonometric functions in equations (13), (14) and (23) become hyperbolic functions and the programme must account for this.)

If it is required to plot the transient solution the various values of $v_s(2\pi/r)$ can be printed out from the computer by substituting a slightly different computer programme. It will be shown in the next subsection however, that to calculate the damping we require just the matrix $[\mathcal{M}]$, where

$$[\mathcal{M}] = \prod_{s=r}^{1} [\mathcal{M}_s]. \tag{26}$$

The values of the elements $[\mathcal{M}]$ depend upon the size of the intervals $\psi_s - \psi_{s-1}$, but converge to a limit as $r$ increases. It is found in practice that for most regions of the $\mu,n$ plane the convergence is such that 30 intervals are adequate to give sufficiently accurate values of the elements.

4.3. *Calculation of the damping.*

We have seen that the solution of equation (9) can be written in the form given by (11)

i.e., $$v(\psi) = \alpha_1 \exp[\gamma\psi].P_1(\psi) + \alpha_2 \exp[-\gamma\psi].P_2(\psi).$$

Let us assume that the initial conditions are such that $\alpha_2$ is zero and $\alpha_1$ is non-zero.

Then $$v(\psi) = \alpha_1 \exp[\gamma\psi].P_1(\psi) \tag{27}$$

and $$v'(\psi) = \alpha_1 \exp[\gamma\psi].[\gamma P_1(\psi) + P_1'(\psi)]. \tag{28}$$

Then as $P_1(\psi)$ is periodic with period $2\pi$, putting $\psi = 0$ and $\psi = 2\pi$ in equations (27) and (28) we have

$$v(0) = \alpha_1 P_1(0) \tag{29}$$

and $$v(2\pi) = \alpha_1 \exp[2\pi\gamma].P_1(0) \tag{30}$$

$$v'(0) = \alpha_1[\gamma P_1(0) + P_1'(0)] \tag{31}$$

and $$v'(2\pi) = \alpha_1 \exp[2\pi\gamma].[\gamma P_1(0) + P_1'(0)]. \tag{32}$$

Equations (29) to (32) can be combined to form the matrix equation

$$[V(2\pi)] = [\Lambda I][V(0)] \tag{33}$$

where $$\Lambda = \exp[2\pi\gamma]. \tag{34}$$

But from equations (24) and (26)

$$[V(2\pi)] = [\mathcal{M}][V(0)]. \tag{35}$$

Using the result proved in Section 4.3 we deduce that $\Lambda$ is given by

$$|\mathcal{M} - \Lambda I| = 0 \tag{36}$$

i.e. the values of $\Lambda$ are given by the latent roots of $[\mathcal{M}]$.

We can then calculate $\gamma$ from equation (34).

In particular as $|\mathcal{M}| = 1$ the latent roots $\Lambda_1, \Lambda_1$ of equation (36) are such that

$$\Lambda_1 . \Lambda_2 = 1$$

i.e.
$$\gamma_1 + \gamma_2 = 0 \text{ or } \gamma_1 = -\gamma_2 .$$

This confirms the result of equation (5), Section 3.2. Having obtained $\gamma$ we can evaluate the damping of the system using the real part of $\gamma$ as shown in Section 4.1.

5. *Results of Section* 4.

In Section 4.1 we found that the form of solution of equation (2) is given by equation (12). In particular the term

$$\beta = \alpha_1 \exp \left[ -\left(\frac{n}{2} - \gamma\right) \psi \right] . P_1(\psi) \exp\left[\tfrac{2}{3} n\mu \cos \psi\right]$$

will give us the information required to determine the nature of the solution. The factor $P_1(\psi) \exp [\frac{2}{3} n\mu \cos \psi]$ is periodic with period $2\pi$ and writing

$$\gamma = \lambda + i\nu$$

it is clear that $\lambda$ effects the damping while $\nu$ indicates the frequency of solution.

5.1. *Frequency of Oscillation in Regions of Destabilization*

In solving the determinantal equation (36) and by virtue of equation (25)

$$\Lambda^2 - (m_{11} + m_{22})\Lambda + 1 = 0 \tag{37}$$

where $m_{ij}$ is the element of the $i^{th}$ row and $j^{th}$ column of matrix $[\mathcal{M}]$.

This leads to the equation

$$\gamma = \frac{1}{2\pi} \log \left[ \frac{(m_{11} + m_{22}) \pm \sqrt{(m_{11} + m_{22})^2 - 4}}{2} \right] . \tag{38}$$

Now Horvay[1] shows two regions of destabilization for low values of $\mu$, one with frequency $\frac{1}{2}$ cycle per revolution and one with frequency 0, and Shutler and Jones[2] indicate a third region with frequency 1 cycle per revolution. In those regions of destabilization where the frequency is unity or zero, $(m_{11} + m_{22}) > 2$, giving real values for $\gamma$. These real values give the damping.

When the solution has a frequency of $\frac{1}{2}$, $(m_{11} + m_{22}) < -2$ and equation (38) can be written

$$\gamma = \frac{1}{2\pi} \log \left[ \frac{-(m_{11} + m_{22}) \pm \sqrt{(m_{11} + m_{22})^2 - 4}}{2} \right] + \tfrac{1}{2} i. \tag{39}$$

The logarithmic term, which is now real, gives the damping and the imaginary part $\frac{1}{2}i$ changes the periodic functions which have period $2\pi$ into periodic functions with period $4\pi$, i.e., frequency of $\frac{1}{2}$ cycle per revolution.

In regions where there is no destabilization

$$|(m_{11}+m_{22})| < 2 \text{ and } \gamma \text{ is then wholly imaginary.}$$

In the investigation of regions of destabilization in the $\mu$, $n$ plane it is helpful to have a datum within each region where the frequency is known. In the present method when $(m_{11}+m_{22}) < 2$, it would not be immediately clear whether the point under investigation was in the region with frequency 1 or that with frequency 0. However, using the previous results[1, 2], where the plane has already been divided up by characteristic curves enclosing regions with known frequency for low values of tip speed ratio, the method described above can be used to extend the curves to higher values of $\mu$. We note that the characteristic curves are the loci of points where $|m_{11}+m_{22}| = 2$.

These curves are shown on Fig. 1, which is the $\mu$, $n$ plane for tip speed ratios up to 1.6 and values of $n$ up to 2.4; the three destabilization regions with frequency 0, $\frac{1}{2}$ and 1 cycles per revolution are clearly shown. In between each such region there is a region where the damping is the same as that for zero tip speed ratio but as $\mu$ increases the area of these regions decreases very rapidly.

5.2. *Degree of Destabilization.*

Having divided the $\mu$, $n$ plane up into destabilized and non-destabilized regions it is necessary to give some measure of the amount of destabilization within the destabilized regions.

Now when $\mu = 0$, i.e. in hovering conditions equation (7) reduces to

$$\beta'' + n\beta' + \beta = 0 \tag{40}$$

which represents a damped periodic motion with damping $-n/2$ if $n < 2$. We take this value of the damping as the norm and introduce the parameter $n_{\text{app}}$ where

$$n_{\text{app}} = n - 2\lambda \tag{41}$$

as the apparent value of $n$ in forward flight with $n_{\text{app}}/2$ being the apparent damping. Clearly the reduction in damping is the amount $\lambda$.

Writing
$$N = \frac{n_{\text{app}}}{n} = 1 - \frac{2\lambda}{n} \tag{42}$$

we see that $N = 1$ when $\lambda = 0$, i.e. when there is no reduction of damping and $N = 0$ when $\lambda = n/2$, i.e. when the motion becomes unstable. Thus $N$ is a measure of the amount of destabilization.

In Fig. 1 curves of constant value of $N$ are plotted in the $\mu$, $n$ plane for values of $n$ up to 2.4 and values of $\mu$ up to $\sqrt{2}$.

5.3. *General Remarks*

From Fig. 1 we can see the effect of increasing the tip speed ratio on the stability of the flapping motion. For current helicopters the value of inertia number $n$ usually lies between 1·4 and 2·0, and we see therefore that initially increasing $\mu$ causes a decrease in stability as an area of destabilization with frequency $\frac{1}{2}$ is entered. As $\mu$ increases further this decrease ceases and the motion becomes more stable until the characteristic curve for the area is again crossed. There is a brief interval of $\mu$ then where this motion has the same degree of stability as in the hovering condition but on increasing $\mu$ further the characteristic curve of the region of destabilization with frequency 1 is crossed and subsequently there is a rapid loss of stability. Finally, the motion becomes unstable for all practical values of $n$ when $\mu \simeq \sqrt{2}$. This value for

$\mu_2$ is confirmed for very small values of $n$ by the work of Shutler and Jones[2] and supporting evidence can be got from the particular integral of equation (1). The forcing function $E(\omega t)$ contains terms with periods of once and twice per revolution so that the particular integral can be evaluated[1] by writing $\beta$ as a Fourier series

$$\beta = a_0 + \sum_{r=1}^{r=\infty} a_r \cos r\psi + \sum_{r=1}^{r=\infty} b_r \sin r\psi .$$

One of the equations for the Fourier coefficients is

$$(1-\tfrac{1}{2}\mu^2)a_1 = -[\tfrac{2}{3}\mu b_2 + \tfrac{1}{2}\mu^2 a_3] + \mu\delta \tag{37}$$

where $\delta$ is a function of the flight conditions. This suggests that when $\mu = \simeq \sqrt{2}$, $a_1$ becomes infinite whatever the value of $n$ which in turn implies that at this value of $\mu$ resonance occurs. It is known that for differential equations with periodic coefficients resonance occurs on the boundary between stable and unstable solutions. However, the occurrence of an equation giving an infinite value for $a_1$ does not in itself prove that the motion is unstable, for this equation is effectively obtained by expanding in powers of $\mu$ and retaining a finite number of terms. This in itself implies that an approximation is being made and that further investigation is required to confirm that instability occurs at $\mu = \sqrt{2}$. The results shown in Fig. 1 provide this confirmation.

For values of $n$ greater than two there is a region of destabilization of frequency 0 for low values of tip speed ratio.

The transient motion for a blade with inertia number of 1·6 is shown for two values of tip speed ratio in Fig. 2. In the first case for $\mu = 0{\cdot}3$ we can see from Fig. 1 that the motion has frequency $\frac{1}{2}$ and is very stable. In fact from Fig. 2 we see that the transient is nearly damped out after one revolution. When $\mu = 1{\cdot}4$, however, the motion has frequency 1, and is very nearly neutrally stable. This is again shown from studying the transient. The general solution consists of two terms, one of which is heavily damped and the other only very slightly damped. The effect of the heavily damped term is lost after about half a revolution and thereafter the motion is nearly periodic with period $2\pi$. This can be seen by comparing the transient between 180° and 360°, and 540° and 720°.

Finally, Fig. 3 compares the results of the method described in this Report with those of Horvay. The region of the $\mu$, $n$ plane shown, is that which is given in detail in Horvay's paper[1], and it can be seen that good agreement is obtained.

6. *Equation of Motion when Allowing for Reverse Flow.*

We now consider the validity of the equation of motion of the rotor blade given by equation (1), for in deriving this the tip speed ratio is assumed to be small.

6.1. *The region of reverse flow.*

The resultant air flow over a helicopter rotor blade can be thought of as consisting of two components, the first being a component due to the forward speed of the helicopter $V$, the second being due to the rotational speed ($\omega$) of the rotor. Fig. 4a shows a rotor blade in two positions, one an advancing position ($0 < \psi < \pi$) and the other a retreating position ($\pi < \psi < 2\pi$) and for either case it can be seen that the resultant airflow perpendicular to the radial direction of the blade is $\omega r + V \sin \psi$. When the blade is in an advancing position this quantity is always positive but if we consider it in a retreating position then the quantity $V \sin \psi$ is negative, and for non-zero $V$ the expression $\omega r + V \sin \psi$ becomes negative for sufficiently small $r$. When this situation arises the resultant flow over the rotor blade is reversed and the area in which this condition occurs is called the region of reverse flow. It is easily shown that this region is a circle with diameter along the line $\psi = 270°$ and length $V/\omega$, one end of which coincides with the rotational centre.

Now for small tip speed ratios $\mu$ these circles are relatively small compared with the area of the rotor disc, and can be neglected with little loss of accuracy. However, as $\mu$ increases the reverse flow area also increases so that for values of $\mu$ greater than unity, the diameter of the reverse flow region is greater than the radius of the rotor disc. Thus the actual physical region of reverse flow is no longer a circle but a portion of circle cut off by the circumference of the rotor disc as shown in Fig. 4b. It can be seen therefore that this region is a considerable proportion of the total rotor disc. We can now divide the rotor disc into four sectors as shown in Fig. 4c. The first sector $OAB$ is one in which there is no reverse flow over any but a small inboard portion of the blade, and the angle of attack of the blade is in the region of 0°. This sector covers all the advancing side of the rotor disc as well as some part of the retreating side. The second sector $OCD$ is one in which the flow is completely reversed and the angle of attack is in the region of 180°. It has been shown[6] that the steady lift curve slope $a$ is constant throughout these regions and has approximately the same value in each of them. It can be assumed therefore that the value of the lift curve slope is constant throughout these sectors.

There are also two smaller sectors $OAC$ and $OBD$ which separate the two already defined, in which the flow is reversed over part of the blade only. In these sectors however the angle of attack is in the region of 90° so that the dominant force on the blade is a drag force, and in addition the resultant velocity of airflow is relatively small. Now forces on the blade are proportional to the square of the velocity, so that the total force acting on the blade in the two small sectors are very small. In addition the area of these sectors diminishes as the tip speed ratio increases, so that we can ignore them with little loss of accuracy.

It will be assumed therefore that for tip speed ratios of unity and higher, the rotor disc can be divided into two sectors, one in which there is no reverse flow over any of the blade and the other in which the flow is reversed over the entire blade. This latter sector is symmetrical about the $\Psi = 270°$ line as shown in Fig. 4b.

Outside the sector of reverse flow the equation of flapping motion will be identical to that derived by Horvay[1]. We make the same assumptions as he does in deriving the equation, namely that the blade is rigid and the flapping hinge is on the axis of rotation and perpendicular to the spanwise axis of the blade. We now derive the equivalent equation which will be valid in the reverse flow sector.
is a circle with diameter along the line $\psi = 270°$ and length $V/\omega$, one end of which coincides with the
flow is reversed over the entire blade. This latter sector is symmetrical about the $\psi = 270°$ line as shown

6.2. *Equation of Motion in Reverse Flow Sector.*

The equation of flapping motion of a rotor blade in the sector of reverse flow can be derived in a similar manner to that given by Horvay[1] for the motion when there is no reverse flow. Only the aerodynamic forces are affected by reverse flow so that the centrifugal force is given by :

$$C = \int_0^R dC = \int_0^R r\omega^2 dm \tag{38}$$

The lift force which now acts downwards (*see* Fig. 5a) is given by

$$\int_0^R dL = \frac{1}{2}\int_0^R \rho c \frac{dC_L}{d\alpha}(\theta - \phi)U^2 dr \tag{39}$$

where $\rho$ is the air density, $c$ the chord, $dC_L/d\alpha$ the slope of the lift curve, $\theta$ the blade pitch angle, $\theta - \phi$ the angle of attack and $U$ the resultant air velocity. It has been shown in Section 6.1 that we can assume that the lift curve slope $a$ is constant over the entire rotor disc with little loss of accuracy. For reverse flow $U$ will be in the direction shown in Fig. 5a.

The longitudinal component of velocity $U_T$ at an element of the rotor blade is

$$U_T = \omega r - \mu\omega R \sin\psi \tag{40}$$

which is always positive in the reverse flow sector because $\sin\psi$ is always negative.

The perpendicular component is given by:

$$U_P = \lambda'\omega R - r\frac{d\beta}{dt} - \mu\omega R\beta\cos\psi \tag{41}$$

where $\lambda'\omega R$ is the difference between the sinking speed of the helicopter and the induced velocity through the rotor disc.

Now the flapping motion of the blade is obtained by equating moments of forces acting on the blade about the flapping hinge to zero and this gives:

$$I_F\frac{d^2\beta}{dt^2} + \int_0^R r dL + \int_0^R \beta r dC = 0 \tag{42}$$

when $I_F$ is the moment of inertia of the rotor blade about the flapping hinge.

If $\theta$ and $\phi$ are small we can write

$$(\theta-\phi)U^2 = \theta U_T^2 - U_P U_T \tag{43}$$

Substituting equations (38), (39) and (43) into (42) and integrating we obtain the equation

$$\frac{d^2\beta}{dt^2} + 2C(t)\frac{d\beta}{dt} + P^2(t).\beta = E(\omega t) \tag{44}$$

where

$$2C(t) = -n\omega[1+\tfrac{4}{3}\mu\sin\omega t] \tag{45}$$

$$P^2(t) = \omega^2[1-\tfrac{4}{3}n\mu\cos\omega t - n\mu^2\sin 2\omega t] \tag{46}$$

and

$$n = \rho\frac{dC_L}{d\alpha}\frac{cR^4}{8I_F}. \tag{47}$$

If we compare this equation with that obtained by Horvay[1] we see that the reverse flow merely has the effect of changing the sign of $n$.

6.3. *The Equation to be Solved.*

We have seen in Section 6.2 that by making certain assumptions the equation of flapping motion of a rotor blade in the reverse flow region differs from that which holds over the remainder of the disc merely by the difference of sign of the parameter $n$. As we are interested in the transient solution therefore our problem is to find a solution to the equation

$$\frac{d^2\beta}{d\psi^2} + 2C(\psi)\frac{d\beta}{d\psi} + P^2(\psi)\beta = 0 \tag{48}$$

where

$$2C(\psi) = \pm n[1+\tfrac{4}{3}\mu\sin\psi] \tag{49}$$

and $$P^2(\psi) = [1 \pm \tfrac{4}{3} n\mu \cos\psi \pm n\mu^2 \sin 2\psi] \tag{50}$$

the negative signs holding in the sector of reverse flow but all signs being positive otherwise.

Thus equation (48) which is the equation to be solved is a second order differential equation with periodic coefficients, but these coefficients are discontinuous at the boundaries of the reverse flow sector due to the sudden change in the sign of $n$ at these particular stations.

## 7. *Method of Solution.*

We now proceed to show how the method of mean coefficients can be applied to solve equation (48) and in particular to find the effective damping of the motion defined by that equation.

### 7.1. *The Form of Solution.*

In general, the term involving $d\beta/d\psi$ in an equation of the type (48) can be eliminated by making the substitution.

$$\beta = e^{-\int C(\psi)d\psi} . V(\psi) \tag{51}$$

and thus reducing the equation (48) to the form

$$\frac{d^2 v}{d\psi^2} + Q(\psi). V = 0. \tag{52}$$

In the particular case of equation (7) the appropriate substitution is given by (8).

In the case of equation (48) however, the coefficients $2C(\psi)$ and $P^2(\psi)$ cannot be defined by a single trigonometric expression for all $\psi$ and therefore we cannot conveniently eliminate the term involving $d\beta/d\psi$ in this case.

However, equation (48) is a linear differential equation with periodic coefficient of period $2\pi$ and therefore has a solution of the form

$$\beta = \alpha_1 e^{\gamma_1 \psi} P_1(\psi) + \alpha_2 e^{\gamma_2 \psi} P_2(\psi) \tag{53}$$

where $\gamma_1$, $\gamma_2$ are constants (not necessarily real) and $P_1(\psi)$, $P_2(\psi)$ are periodic functions with period $2\pi$. $\alpha_1$, $\alpha_2$ are arbitrary constants depending on initial conditions.

If we write $\gamma_i = \lambda_i + iv_i$ it is seen that the least negative of $\lambda_1$ and $\lambda_2$ gives the parameter by which the damping of the motion can be measured and in particular the motion will be stable if both $\lambda_1$ and $\lambda_2$ are negative but unstable if either are positive. It is the evaluation of these quantities therefore which is our primary aim.

### 7.2. *Rectangular Ripple Principle.*

Section 5 gives a detailed account of the application of this principle to an equation of type (52) so that this section will give only an outline of the method to be used to solve equation (48) emphasising the points where differences occur.

We divide one revolution of $\psi$ into small intervals $\psi_s - \psi_{s-1}$ over which the coefficients $2C(\psi)$ and $P^2(\psi)$ are assumed constant. Values of $\beta$ and $d\beta/d\psi$ must be continuous throughout successive intervals, and the initial values of these quantities for a given interval are taken to be the final values of the previous interval. We choose the number of intervals so that the radial boundaries of the reverse flow region coincide with the division of intervals.

We approximate equation (48) by a set of equations whose coefficients $2C$ and $P^2$ are fixed throughout each of the intervals $\psi_s - \psi_{s-1}$. The values of $2C$ and $P^2$ for each interval are obtained by substituting the mean value of $\psi$ for the interval in $2C(\psi)$ and $P^2(\psi)$ respectively. For intervals in the reverse flow sector the negative signs in equations (49) and (50) are taken, otherwise the positive signs are taken.

Assuming $2C$ and $P^2$ are constant, equation (48) has a solution

$$\beta(\psi) = e^{-C\psi}(A\cos f\psi + B\sin f\psi) \tag{54}$$

where
$$f = (P^2 - C^2)^{\frac{1}{2}} \tag{55}$$

and $A$ and $B$ are constants determined from initial condition for each interval.

From equation (54) we have

$$\frac{d\beta}{d\psi} = \beta'(\psi) = -e^{-C\psi}(A[C\cos f\psi + f\sin f\psi] + B[C\sin f\,\psi - f\cos f\psi]) \tag{56}$$

Equations (54) and (56) can be expressed by the matrix equation

$$[\mathscr{B}(\psi)] = [M(\psi)]\,[D] \tag{57}$$

where
$$[\mathscr{B}(\psi)] = \begin{bmatrix} \beta(\psi) \\ \beta'(\psi) \end{bmatrix}$$

$$[M(\psi)] = [e^{-C\psi}]\begin{bmatrix} \cos f\psi & \sin f\psi \\ -C\cos f\psi - f\sin f\psi & -C\sin f\psi + f\cos f\psi \end{bmatrix}$$

and
$$[D] = \begin{bmatrix} A \\ B \end{bmatrix}.$$

If we divide one revolution into $r$ equal intervals of magnitude $\frac{2\pi}{r}$ the mean value for the $s$th interval is $(2s-1)\frac{\pi}{r}$. $2C_s$ and $P_s^2$, the value of $2C$ and $P^2$ for the $s$th interval are calculated using this value of $\psi$ and the values of $\beta$ and $\beta'$ in that interval are given by

$$[\mathscr{B}_s(\psi)] = [M_s(\psi)]\,[D_s] \tag{58}$$

Using this notation and proceeding as in Section 5.2 we can derive the equation

$$[\mathscr{B}(2\pi)] = \left[\mathscr{B}_r\left(\frac{2\pi}{r}\right)\right] = \prod_{s=r}^{1}\left[M_s\left(\frac{2\pi}{r}\right)\right]\left[M_s(0)\right]^{-1}\cdot\left[\mathscr{B}_1(0)\right] \tag{59}$$

where the order multiplication is such that the product starts with $s = r$ and ends with $s = 1$.

Now
$$[M_s(0)] = \begin{bmatrix} 1 & 0 \\ -C_s & f_s \end{bmatrix}$$

so that $$[M_s(0)]^{-1} = \begin{bmatrix} 1 & 0 \\ C_s/f_s & 1/f_s \end{bmatrix} .$$

Hence

$$[\mathscr{M}_s] = \left[e^{\frac{-2C_s\pi}{r}}\right] \begin{bmatrix} \cos\frac{2\pi f_s}{r}+\frac{C_s}{f_s}\sin\frac{2\pi f_s}{r} & \frac{1}{f_s}\sin\frac{2\pi f_s}{r} \\ -f_s\sin\frac{2\pi f_s}{r}-\frac{C_s^2}{f_s}\sin\frac{2\pi f_s}{r} & \frac{-C_s}{f_s}\sin\frac{2\pi f_s}{r}+\cos\frac{2\pi f_s}{r} \end{bmatrix} \tag{60}$$

where $$[\mathscr{M}_s] = \left[M_s\left(\frac{2\pi}{r}\right)\right] [M_s(0)]^{-1}$$

Thus $$[\mathscr{B}(2\pi)] = \prod_{s=r}^{1} [\mathscr{M}_s].[\mathscr{B}(0)] \tag{61}$$

Hence we see that $\beta(2\pi)$ and $\beta'(2\pi)$ can be calculated in terms of $\beta(o)$ and $\beta'(o)$ by process of evaluating a series of matrix products involving the $C_s$'s and $f_s$'s. These are calculated and the matrices formed and multiplied using a digital computer. (If the quantity $P^2-C^2$ is negative the trigonometric functions in equations (54), (56) and (60) become hyperbolic functions and the computer programme accounts for this.)

If it is required to plot the transient solution, the various values of $\beta_s(2\pi/r)$ can be printed out by substituting a slightly different programme, but it has been shown in Section 4.3 that to calculate the damping we require just the matric $[\mathscr{M}]$ where

$$[\mathscr{M}] = \prod_{r=s}^{1} [\mathscr{M}_s] \tag{62}$$

for the values of $e^{2\pi\gamma_1}$ and $e^{2\pi\gamma_2}$ are the latent roots of this matrix. Hence the damping which is determined by the real parts of $\gamma_1$ and $\gamma_2$ can be found from the matrix $[\mathscr{M}]$.

8. *Results of Section 7.*

From the latent roots of the matrix $[\mathscr{M}]$ in equation (62) not only can the effective damping be found as previously shown but also the frequency of oscillation of the transient flapping. The latter is deduced from the imaginary part of $\gamma_1$ and $\gamma_2$.

8. 1. *Frequency of Oscillation.*

The latent roots of the matrix $[\mathscr{M}]$ can be real and positive, real and negative or complex in nature. If the quantities $e^{2\pi\gamma_1}$ and $e^{2\pi\gamma_2}$ are real and positive then $\gamma_1, \gamma_2$ are also real. Thus from equation (53) we see that in this case each term in the transient solution represents a damped oscillation with frequency one cycle per revolution.

If however $e^{2\pi\gamma_1}$ and $e^{2\pi\gamma_2}$ are negative quantities, say $-\Lambda_1$, $-\Lambda_2$, then

$$\gamma_j = \tfrac{1}{2}\log_e[-\Lambda_j] = \tfrac{1}{2}\pi\log_e\Lambda_j+\tfrac{1}{2}i, \quad j = 1, 2 \tag{63}$$

In this case the damping is given by $\frac{1}{2}\log_e\Lambda_j$ and the imaginary part $\frac{1}{2}i$ changes the periodic function $P_1(\psi)$, $P_2(\psi)$ in equation (53) to periodic functions with period 4, i.e. frequency $\frac{1}{2}$ cycle per revolution.

If $e^{2\pi\gamma_1}$, $e^{2\pi\gamma_2}$ are themselves complex then $\gamma_1$, $\gamma_2$ are also complex and neither the real nor imaginary parts have constant values when this is so.

In presenting the results of the calculations made using the method of Section 7, we consider the variation of $\mu$ and $n$ on the value and nature of $e^{2\pi\gamma}$. We can divide the $\mu$, $n$ plane into regions where the frequency of oscillation is $\frac{1}{2}$, 1 and a third region where the frequency varies between $\frac{1}{2}$ and 1. This is shown in Fig. 6 where the continuous lines forming the boundaries of these regions show where the latent roots of $[\mathscr{M}]$ change from real to complex quantities. Also in this diagram the lines of constant damping within constant frequency regions, are shown.

8.2. *General Remarks.*

Fig. 6 shows the variation of damping over a range of $\mu$ from 1 to 2·8 and $n$ from 0 to 2·4. The regions in which the motion has frequency $\frac{1}{2}$ and 1 are marked and it is seen that these cover most of the $\mu$, $n$ plane shown. For $n > 1{\cdot}2$ as $\mu$ increases past unity the damping decreases slightly at first and then starts to increase until the boundary of the frequency $\frac{1}{2}$ region is reached. There is then a very short interval of $\mu$ where the frequency changes from $\frac{1}{2}$ to 1 and then the damping decreases steadily until the motion becomes unstable at values of $\mu$ between 2·2 and 3·0, depending on value of $n$.

If we compare this figure with that of Fig. 1 we see that the general effect of taking reverse flow into account is to 'stretch' the boundaries of constant frequency regions to the right and this means in turn that the values of $\mu$ for which the motion becomes unstable are higher.

Fig. 7 shows the transient motion of a rotor blade for two revolutions of $\psi$ for an inertia number $n$ of 1·6 and tip speed ratio of 1·4 with and without allowance for reverse flow. As would be expected these motions are identical until the reverse flow region is entered at $\psi = 210°$. However, when reverse flow is ignored the motion has very small effective damping and a frequency of 1 cycle per revolution, but when reverse flow is accounted for the motion has relatively large effective damping and a frequency of $\frac{1}{2}$. This naturally makes considerable difference to the transient motion. To explain the difference in the motion from a physical point of view, we note that in the case where reverse flow is ignored the blade enters a region where the damping becomes negative at azimuth angles of $220° - 230°$. Consequently the amplitude of $\beta$ starts building up from this point and only decreases when positive damping which occurs again at 310°–320°, takes effect. If we take into account reverse flow, however, the region of negative damping becomes a region of large positive damping so that the amplitude of $\beta$ rapidly decreases from 220°–230° onwards.

Fig. 8 shows the transient motion for $n = 1{\cdot}6$ and $\mu = 2{\cdot}4$ i.e. for a value of $\mu$ just below that for which the motion becomes unstable. Here the frequency is 1 cycle per revolution, and the transient solution, which has two terms, contains one which is heavily damped and another which is only slightly so. The effect of the heavily damped term is lost after about half a revolution and thereafter the motion is nearly periodic with period $2\pi$.

Physically the large increase in amplitude of $\beta$ from $\psi = 180°$ onwards is explained by the fact that the stiffness in the quadrant $90° < \psi < 180°$ is negative so that large amplitudes would follow this region.

9. *Conclusions.*

The method of solving the equation of flapping motion of a helicopter rotor blade described in this Report is one which leads directly to the parameter which measures the stability of the motion. In doing this the necessity of plotting a solution is avoided although this can be done with little extra labour. Moreover, the customary numerical methods of solving differential equations such as the Runge-Kutta type do not lend themselves to equations with periodic coefficients whose values fluctuate rapidly.

The results obtained in this Report show that the onset of instability of the blade flapping motion occurs at tip speed ratios in the range of 2·2 to 2·8 for values of inertia number up to 2, when reverse flow over the retreating blade is taken into account. In comparing these results with those obtained by neglecting reverse flow it is found that the onset of instability is delayed until higher tip speed ratios are reached. In allowing for reverse flow it has been assumed that the blade at any time is either entirely within or entirely without this region of reverse flow. The justification for this assumption made in Section 6 is that the portion of the rotor disc in which this is not so is relatively small, and that the forces on the blade under these conditions are also small. This is particularly true for the higher tip speed ratios considered and it is here that the instability occurs. It is reasonable to assume therefore that these results give a true indication of the direct effect of reverse flow on the onset of instability.

These results are in general agreement with those of Wilde, Bramwell and Summerscales[7] who have investigated the problem using an analogue computer. In their work, account is taken of the fact that in the 'partial reverse flow region' airflow is from the leading edge to trailing edge over the outboard part of the blade, but from trailing edge to leading edge over the inboard part. This refinement however, does not appear to lead to any major differences from the results obtained by this report.

Jenny, Arcidiacono and Smith[8] have also investigated the problem, making assumptions similar to those made by Wilde, Bramwell and Summerscales, and deduce that instability occurs at approximately the same value of tip speed ratio.

However, in all these investigations no account has been taken of the elasticity of the blade and the effects due to bending and twisting have been neglected. It is possible that for high tip speed ratios considered the effect of twisting may be particularly marked due to the fact that on entering the reverse flow region the flexural axis of the blade is shifted from the quarter chord to the threequarter chord position.

It would appear, therefore, that the effects of elasticity should be considered and it should be possible to extend the method described in this Report to allow for this.

## LIST OF SYMBOLS

| | |
|---|---|
| $a$ | Slope of blade lift curve |
| $c$ | Blade chord |
| $I$ | Blade moment of inertia about flapping hinge |
| $n$ | Inertia number $= \frac{\rho a c R^4}{8 I_F}$. |
| $n_{app}$ | Apparent value of $n$, $\mu > 0$ |
| $N$ | $n_{app}/n$ |
| $P_i(\psi)$ | Periodic functions of $\psi$ |
| $R$ | Tip radius |
| $t$ | Time |
| $U$ | Resultant air velocity perpendicular to radial direction of blade |
| $U_T$ | Component of U parallel to plane of rotor disc. |
| $U_P$ | Component of U perpendicular to plane of rotor disc |
| $V(\psi)$ | $\beta(\psi) \exp \left[\frac{n}{2} \psi - \frac{2}{3} n \mu \cos \psi\right]$ |
| $\beta(\omega)$ | Flapping angle. |
| $\gamma_i$ | Exponents in solution of flapping angle |
| $\theta$ | Blade pitch angle |
| $\lambda'$ | Difference between sinking speed and induced air velocity, divided by $\omega R$ |
| $\lambda_i$ | Real part of $\gamma_i$. |
| $\Lambda_i$ | $\exp [2\pi\gamma_i]$ |
| $\mu$ | Tip speed ratio |
| $\nu_i$ | Imaginary part of $\gamma_i$. |
| $\rho$ | Density of air |
| $\psi$ | Azimuth angle $= \omega t$ |
| $\omega$ | Rotational frequency of blade |

## REFERENCES


| *No.* | *Author(s)* | *Title, etc.* |
|---|---|---|
| 1 | G. Horvay .. .. .. | Rotor blade flapping motion. *Quart. appl. Maths.*, July, 1947. |
| 2 | A. G. Shutler and J. P. Jones .. | The stability of rotor blade flapping motion. A.R.C., R. & M. No. 3178 May, 1958. |
| 3 | G. Horvay and S. W. Yuan .. | Stability of rotor blade flapping motion when the hinges are tilted. *J. Aeronaut. Sci.*, October, 1947. |
| 4 | O. J. Lowis .. .. .. | The stability of Helicopter rotor blade flapping motion at high tip speed ratios. M.Sc. Thesis University of Southampton, 1963. A.R.C. 23371, January, 1962. |
| 5 | N. W. McLachlan .. .. | *The theory and application of Mathieu functions.* Oxford University Press, 1947. |
| 6 | A. Gessow and A. D. Crim .. | A method for studying the transient blade flapping behaviour of lifting rotors at extreme operating conditions. NACA T.N. 3366, January, 1955. |
| 7 | E. Wilde, A. R. S. Bramwell, and R. Summerscales .. .. .. | The flapping behaviour of a helicopter rotor at high tip speed ratios. A.R.C., C.P. 877, April, 1965. |
| 8 | D. S. Jenny, P. J. Arcidiacono and A. F. Smith. .. .. .. | A linearized theory for the estimation of helicopter rotor characteristics at advance ratios above 1·0. *Proceedings of the Ninth Annual National Forum of the American Helicopter Society*, May, 1963. |

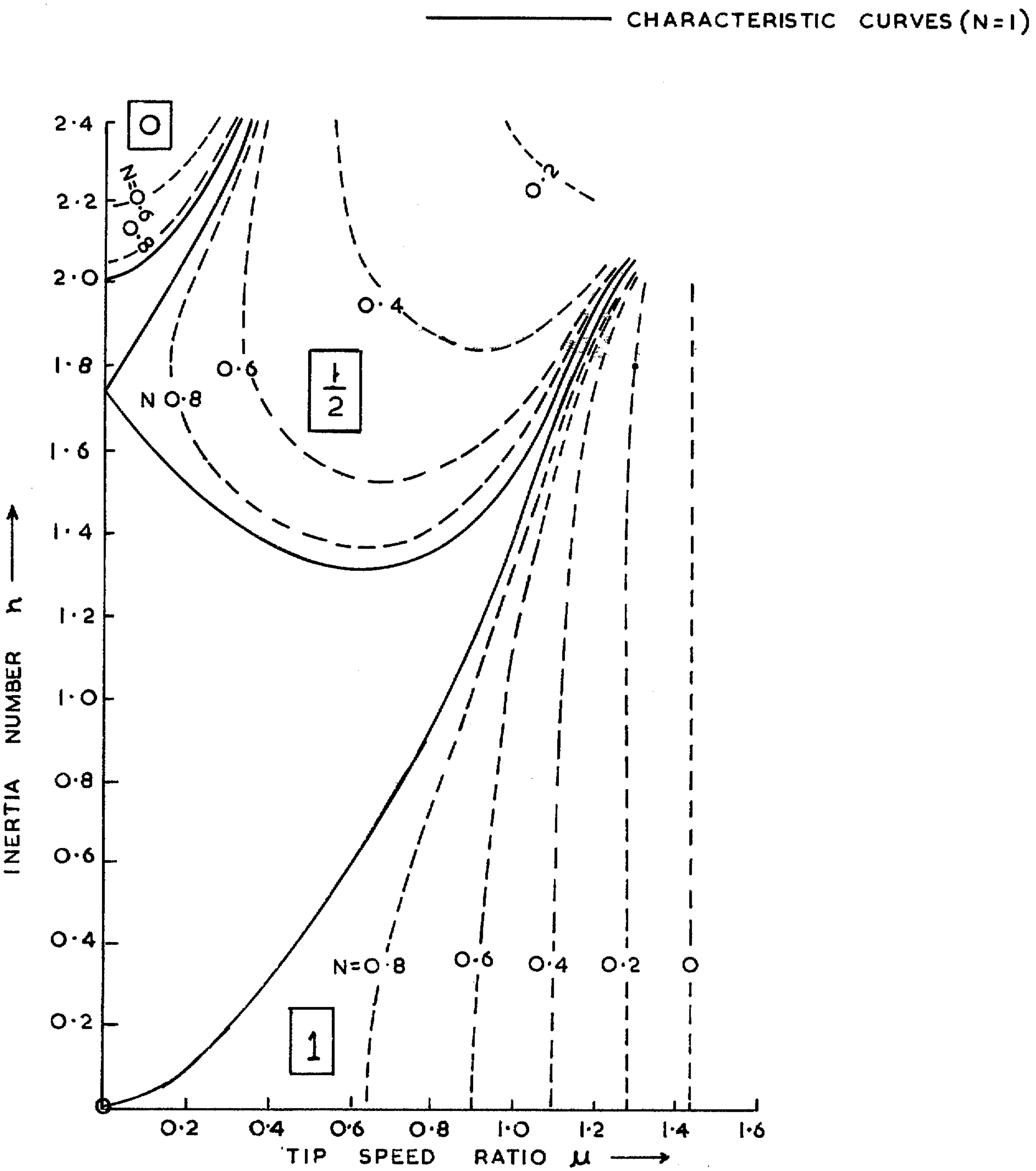


FIG. 1. Rotor blade stability diagram.

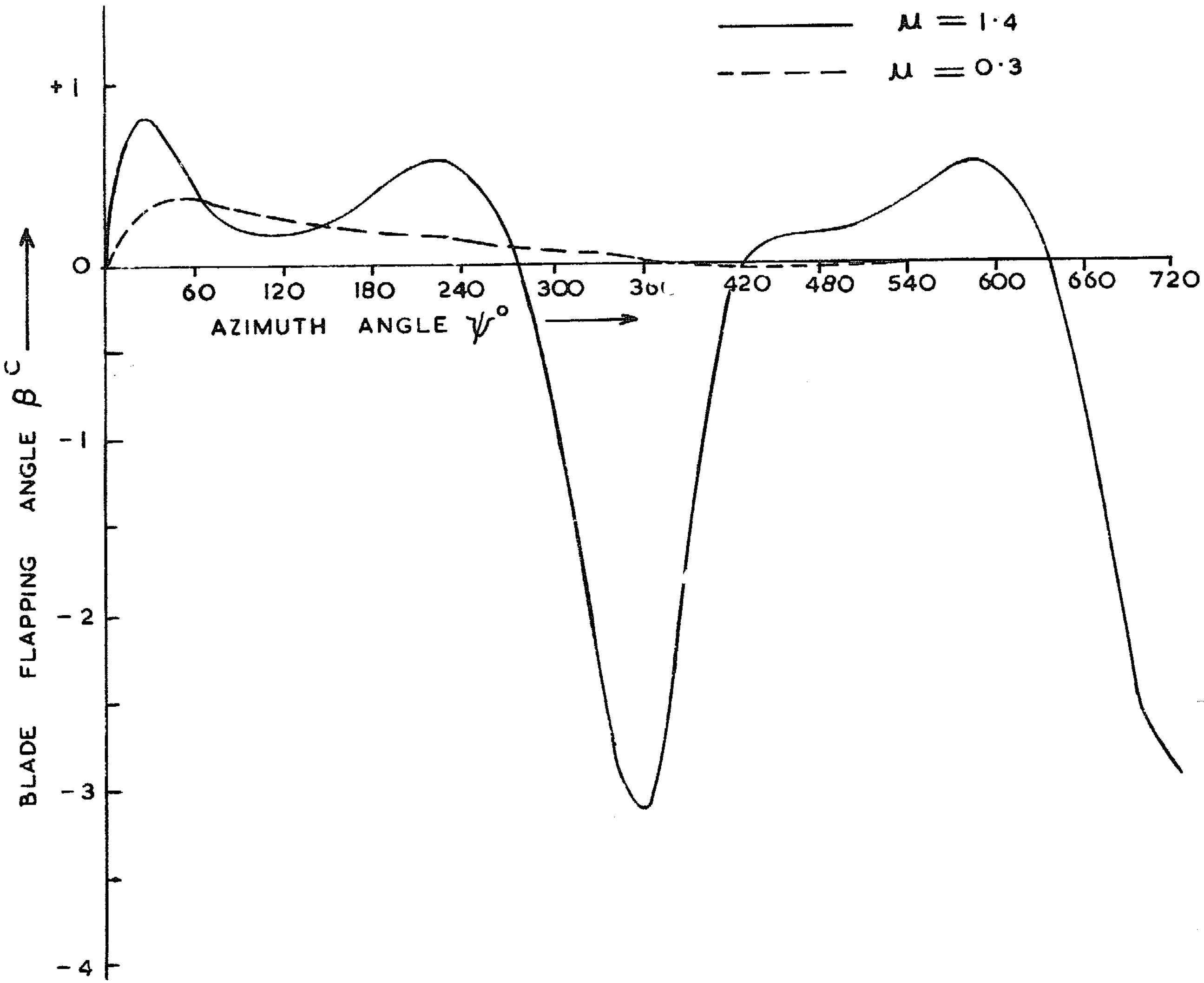


FIG. 2. Flapping transients for $n = 1{\cdot}6$. $\beta(0) = 0$, $\beta'(0) = 1$.

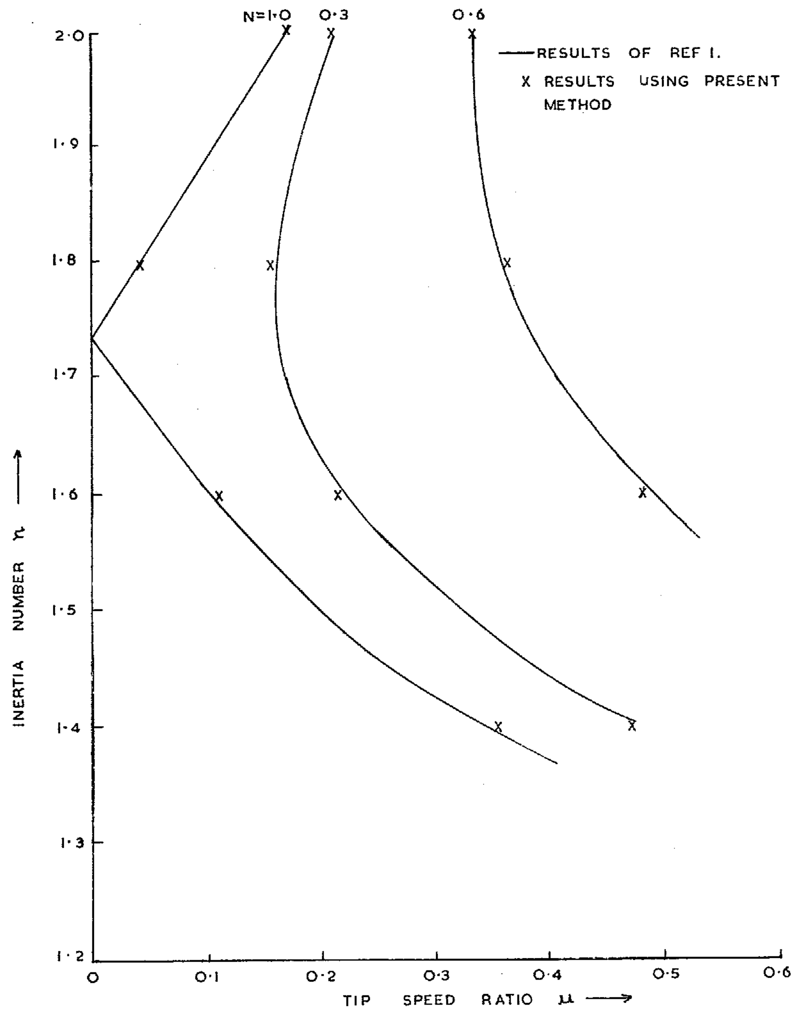


FIG. 3. Comparison of results with those of Reference 1.

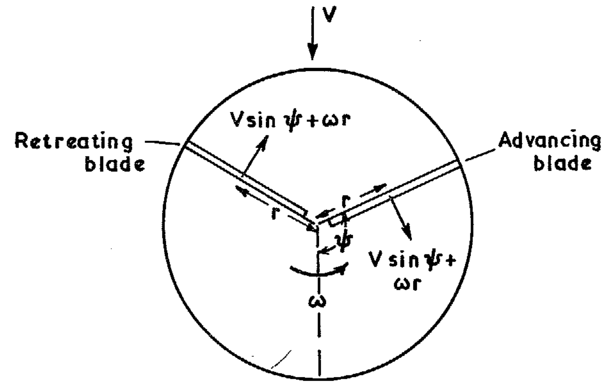


FIG. 4a. Resultant velocities over the rotor disc.

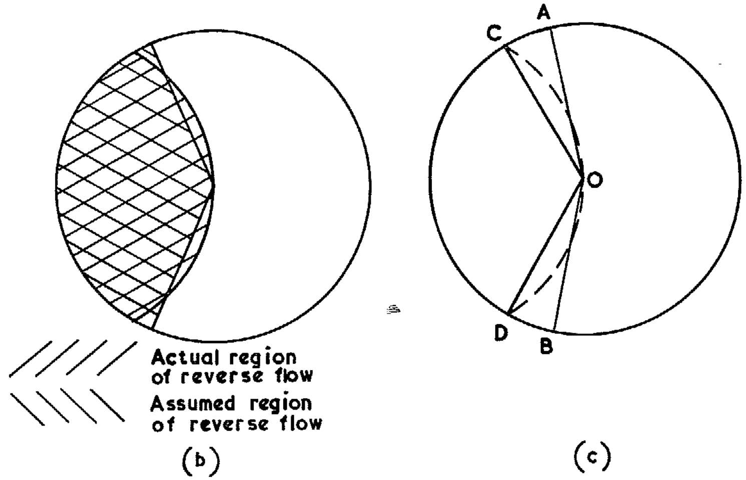


FIG. 4b & c. Reversed flow region.

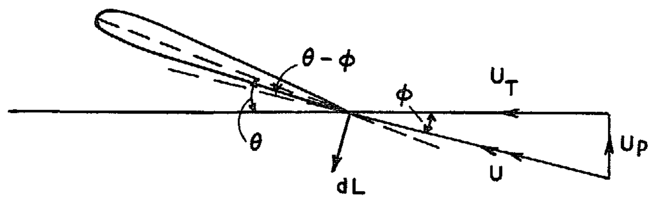


FIG. 5a. Velocities at blade element for reverse flow region.

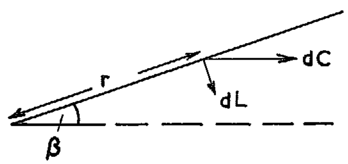


FIG. 5b. Forces at blade element for reverse flow region.

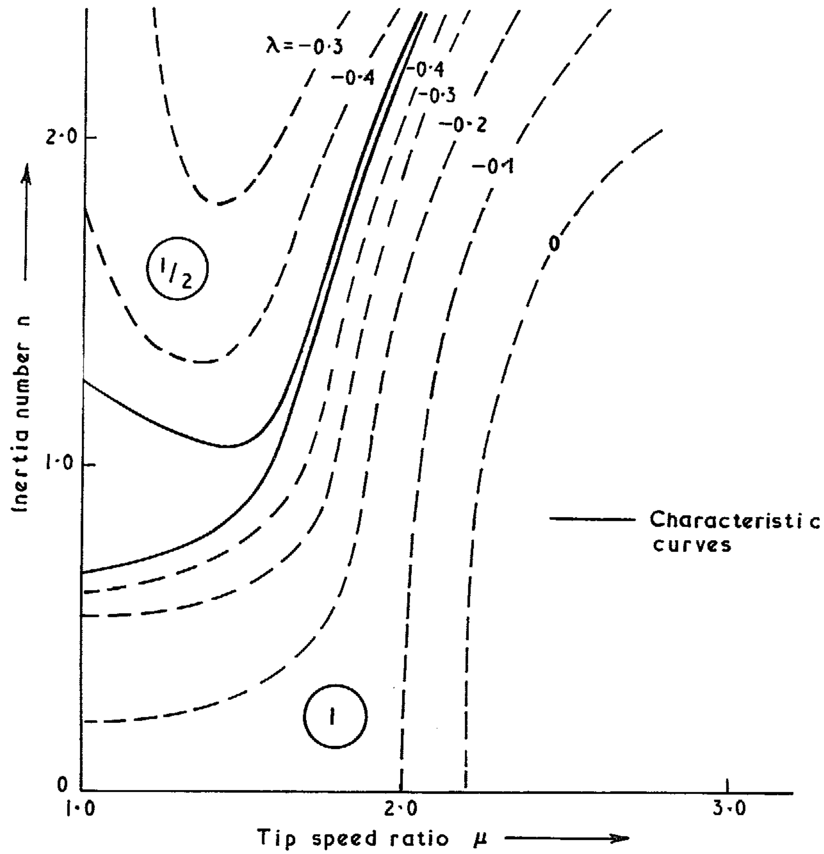


FIG. 6. Rotor blade stability diagram.

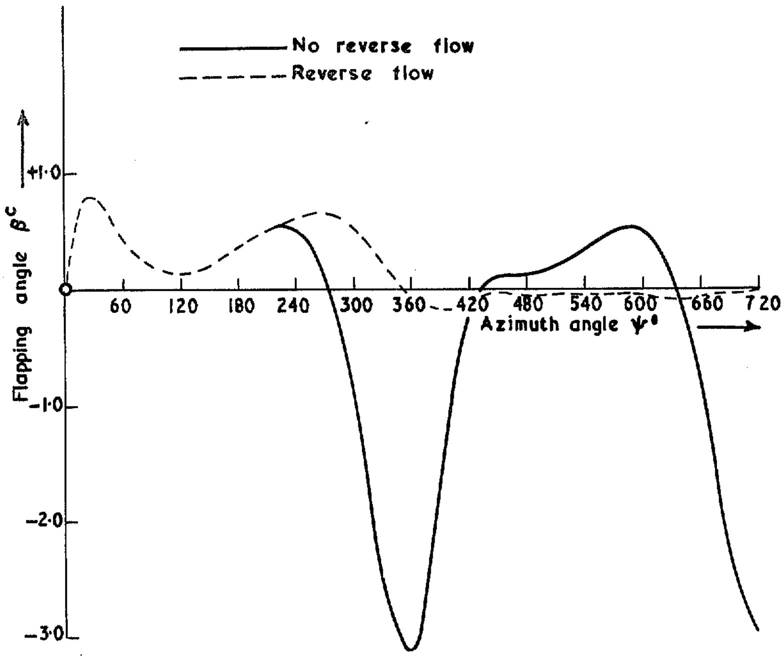


FIG. 7. Flapping transient for $n = 1{\cdot}6$ $\beta(0) = 0$, $\beta'(0) = 1$ at $\mu = 1{\cdot}4$.

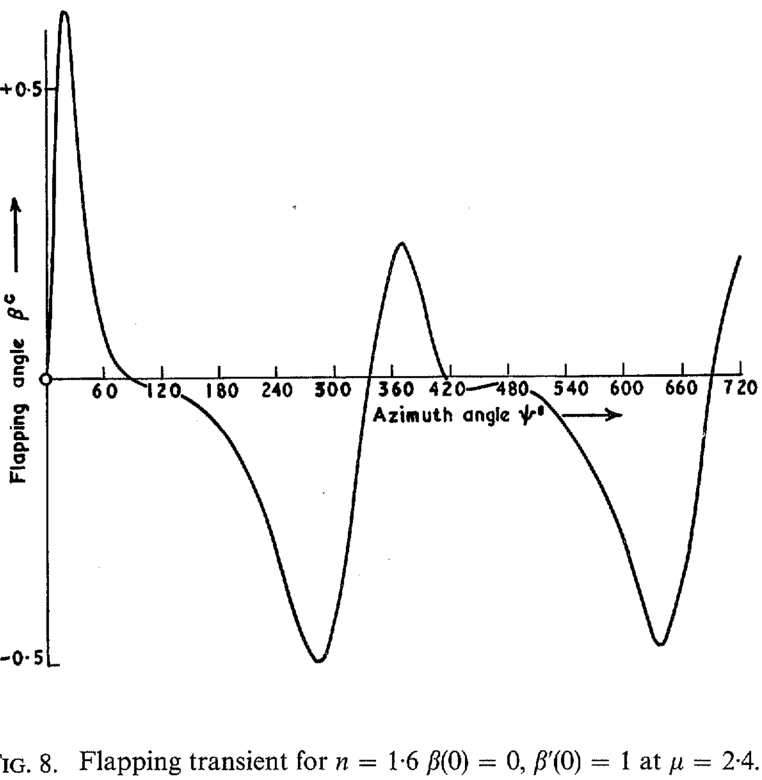


FIG. 8. Flapping transient for $n = 1{\cdot}6$ $\beta(0) = 0$, $\beta'(0) = 1$ at $\mu = 2{\cdot}4$.


Printed in Wales for Her Majesty's Stationery Office by Allens Printers (Wales) Limited

Dd.129527 K.5

R. & M. No. 3544



Published by
HER MAJESTY'S STATIONERY OFFICE

To be purchased from
49 High Holborn, London W.C.1
423 Oxford Street, London W.1
13A Castle Street, Edinburgh 2
109 St. Mary Street, Cardiff CF1 1JW
Brazennose Street, Manchester 2
50 Fairfax Street, Bristol 1
258–259 Broad Street, Birmingham 1
7–11 Linenhall Street, Belfast BT2 8AY
or through any bookseller

R. & M. No. 3544

S.O. Code No. 23–3544